DMD2020-9077

DESIGN AND OPTIMIZATION OF PATIENT-SPECIFIC PEDIATRIC LARYNGOSCOPES

Madelene Habib, Robert Sims, James Inziello, Fluvio Lobo[1], Jack Stubbs
University of Central Florida, Institute for Simulation and Training
Orlando, Florida, USA

ABSTRACT

Pediatric laryngoscope blades do not vary in size and shape as patients' airways do. Difficult airway intubations may require physicians to try different blade sizes and even improvise. In addition to physical trauma and complications, difficult intubations may result in longer operating room times. As advanced three-dimensional (3D) imaging, modeling, and printing technologies become more ubiquitous at the point-of-care, so will the development and fabrication of patient-specific solutions. Here we introduce a method for the design and fabrication of patient-specific, single-use pediatric laryngoscope blades. The process seeks to optimize procedures and mitigate complications by providing physicians with the right tool at the right time.

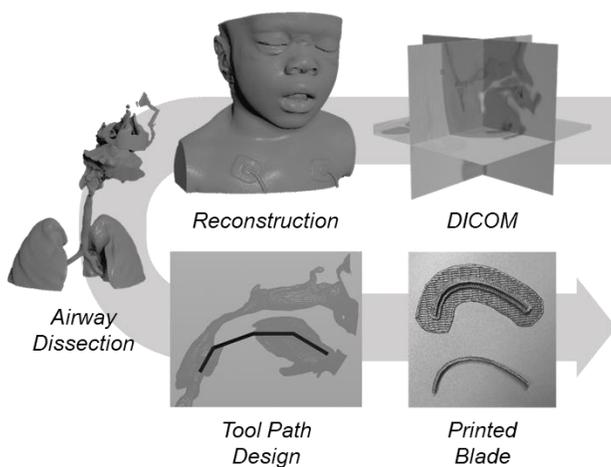Keywords: Pediatrics, Airway, Intubation, Laryngoscopes, Patient-Specific, 3D Printing

FIGURE 1: PROCEDURAL ALGORITHM FOR THE DESIGN OF PATIENT-SPECIFIC LARYNGOSCOPES

[1] Contact author: flobo@ist.ucf.edu

INTRODUCTION

Pediatric laryngoscopes did not exist until the late 1940s. Tactile methods were used by anesthetists until 1946 when a variation of the Miller blade was modified to fit pediatric patients [1]. Laryngoscope modifications have been addressing challenging airways thereafter. A few laryngoscopes today include the Glidescope Spectrum, Airtraq, and the McGrath Blade all featuring disposability, varied sizes, optics, and video screens [2]. Mandatory high-level disinfection requirements on reusable laryngoscopes has motivated the use of disposable blades, ultimately lowering costs [3]. Variability in size is also critical when choosing blades. However, for pediatric intubation, there is a lacking in variable blade sizes as current laryngoscopes include one size for neonates, and one size for pediatrics [4]. Sizes match a range of endotracheal tube sizes (2.5-3.5 for neonate, and 4.0-5.5 for pediatrics) [2]. Infants and children have diverse anatomical structures within their own age groups and could be the leading cause of neonates having the highest risk of intubation complications for both normal and abnormal airways [5]. Advancements in three-dimensional (3D) imaging, modeling, and printing can allow physicians to create patient-specific devices at the point-of-care, reducing any risks in difficult airway intubation. Here we introduce a semi-automated, consolidated approach for the design and fabrication of patient-specific, single-use laryngoscope blades (Figure 1).

METHODS
Patient Data

De-identified computed tomography (CT) datasets from fifteen (15) cases were obtained from Nemours Children's Hospital (Lake Nona, FL, USA). Age, weight, and height were also retrieved for each case when available. Nemours' health professionals anonymized all case data retrieved. Case information was summarized in Table 1. Data retrieval and analysis protocols were vetted by UCF's IRB office.

| TABLE 1: CASE SUMMARY			
Case	Age (months)	Weight (Kgs.)	Height (cm.)
12	2	5.3	54.0
8	3	5.5	59.0
11	6	3.8	40.0
18	12	9.0	N/A
10	17	15.7	90.0
19	17	N/A	N/A
9	33	15.8	93.6
22	33	13.2	N/A
21	34	11.5	89.9
23	36	11.6	89.6
20	38	17.2	96.5
15	60	17.8	91.4
16	91	23.6	123.0
13	108	20.6	118.1
7	N.A.	N.A.	N.A.

Patient-Specific Procedural Design Platform

We developed a set of algorithms in Houdini 17 (Side Effects Software Inc., Toronto, CA), to: (1) Read and Reconstruct Digital Imaging and Communication in Medicine (DICOM) datasets, (2) Isolate the airway passage, (3) Outline a path from the oral cavity to the epiglottis, and (4) Construct a patient-specific, 3D printable laryngoscope blade (Figure 1).

Reconstruction

CT datasets were reconstructed using a custom Houdini-based procedural network. Reading DICOM data relied on Pydicom, a Python package for the manipulation of digital medical imaging [6]. Additional Python modules were built to normalize and pad the imported data. Normalization functions mapped each CT's native Hounsfield range to a 0-1 scale. Padding functions surround the DICOM dataset with empty voxels to ensure that the reconstruction process results in a closed geometry. Finally, a 3D reconstruction was generated by setting an intensity threshold of 0.2 (20%). Voxels with normalized intensity values >0.2 were set to 1 (100% intensity). Anything below the threshold was set to 0. The resulting voxel-based reconstruction could be best described as a homogenous volume encompassing all tissue, soft and rigid.

Dissection of the airway was achieved through voxel morphology and shrink-wrapping. First, the voxel-based reconstruction was dilated until internal structures, such as the airway, disappeared (Figure 2.A-B). The resulting volume enclosed (or wrapped) around the original reconstruction (Figure 2.C). Each point composing the dilated volume was then projected, along its normal, towards the enclosed reconstruction. This operation resulted in a volume absent of an airway (Figure 2.D). Openings, sharp curves, and other surface details are lost to a crude interpolation between projected points, which resembles the use of shrink-wrap (Figure 2.D). Finally, the reconstruction was subtracted from the shrink-wrapped volume. The operation produced several independent volumes, including the airway (Figure 2.E). Although our method can automatically select the airway based on size, the user can also select one or more volumes manually. Selected volumes are then merged to form the extracted patient airway (Figure 2.F).
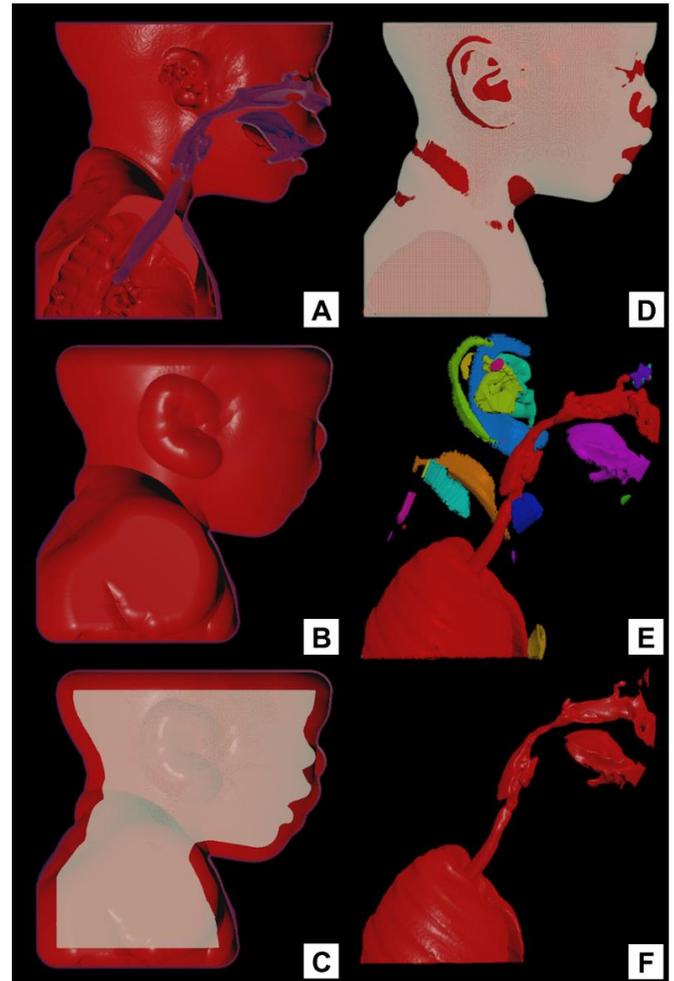
FIGURE 2: AIRWAY DISSECTION THROUGH VOXEL MORPHOLOGY AND SHRINKWRAPPING

Patient-specific laryngoscope blades were designed from build paths conformed to extracted airway volumes. Build paths were constructed using two variants of the space colonization algorithm (SCA) introduced by Runions et al. [7]. SCAs generate a sequence of points that follow the calculated average direction of a point cloud composing a volume or region of interest. Our method generates a point cloud from the voxels comprising the extracted airway volume. Point clouds superior to the oral cavity (nasopharynx) and inferior to the epiglottis (trachea, bronchi, and lungs) were removed manually to improve performance. Given a starting point within the most anterior region of the oral cavity, both SCA variants constructed a path to the epiglottis (Figure 3). SCA variants were modified to record the position of nearest and furthest point on each iteration. Both methods also recorded the length of the path, which was then used to compare against the industry standard.

Build paths constructed with both SCA variants were fitted to a quadratic equation of the form;

$$y = Ax^2 + Bx + C \qquad (1)$$

The curvature (A), the height or *y*-intercept (C), and the symmetry (B and -B/2A) of the parabola were recorded for each case. Model fitting was done with three goals: (1) Ensure a smooth path for fabrication, (2) Correlate model parameters to age, weight, and/or height changes across the patient population, (3) Compare patient-specific laryngoscopes to commercially-available options.

Finally, the L-shaped profile seen in standard laryngoscope blades was swept along the patient-specific build path to form a 3D model of a blade for fabrication. The model was exported as a .STL and .OBJ file for 3D printing (Figure 1). Fabrication of patient-specific blades was done for demonstration purposes only.
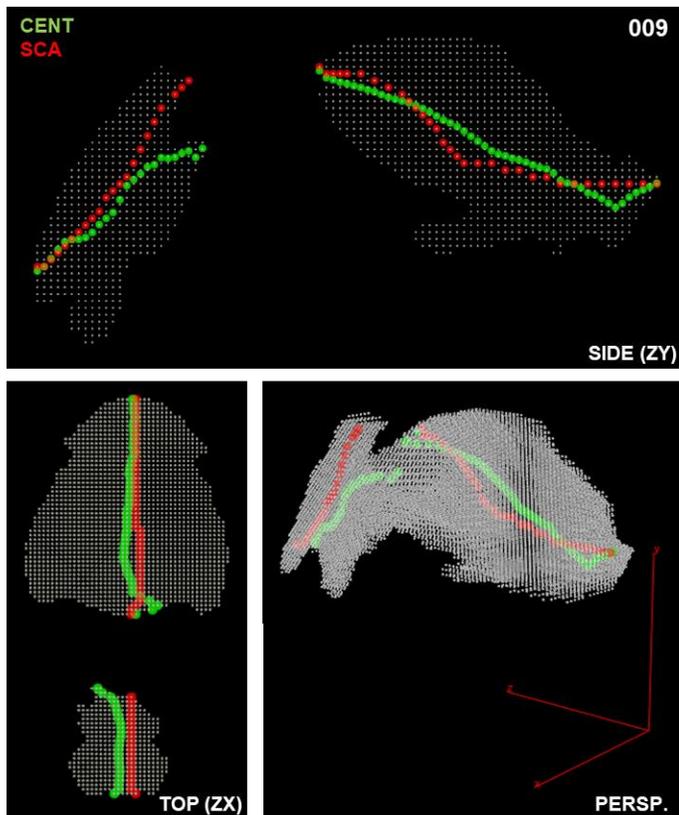

FIGURE 3: BUILD PATHS

RESULTS AND DISCUSSION

Our custom automated reconstruction produced volumes of quality comparable to industry standard programs (e.g. Slicer, Mimics). The method uses Pydicom, a trusted Python library for DICOM manipulation [6]. While no direct comparison was shown here, our team used Slicer to corroborate the accuracy of our automated method. As we will discuss later, some cases were not used due to the nature of the CT dataset. Future work will include a quantitative analysis between our method and Mimics,

the industry standard. Our automated method generated voxel-based reconstructions with a resolution of 0.1 mm/voxel.

Shrink-wrapping as means of dissecting internal structures seeks to automate an otherwise manual process. Reconstructing the airway using Slicer or Mimics is not difficult, just time consuming. Manual operations are required, leading to inter-operator inconsistencies. Two parameters currently control the shrink-wrapping process: (1) the magnitude of the dilation and (2) the number of independent volumes that constitute the airway. On average, reconstructions were dilated by 22.78 voxels or 2.28 millimeters (μ = 2.28, s = 0.44, N = 15). In most cases, the oral cavity and larynx were reconstructed as independent volumes. Selecting the volumes corresponding to the airway was therefore left as a manual input in our method.

Our method currently relies on the presence of air in the oral cavity to establish a build path for the laryngoscope blade which air speeds the reconstruction process, but reduces the number of usable datasets. Some cases were omitted from this study due to the absence of air in the oral cavity. Future iterations of our method will address this issue by relying on anatomical features and compartments (e.g. bones, nasopharynx).
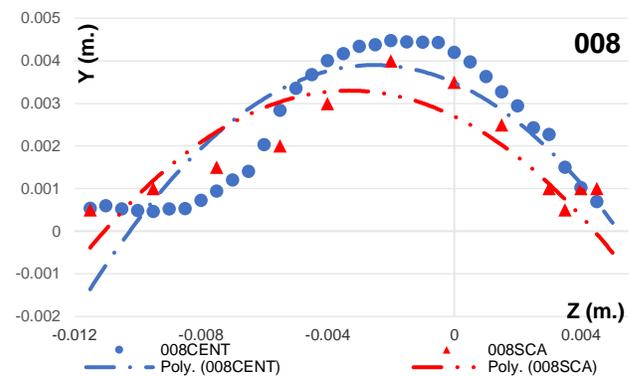

FIGURE 4: QUADRATIC FIT TO BUILD PATHS

SCA variants were effective at calculating a path between the patient's mouth and the epiglottis, but require improvements to measure width and height of the airway passage. SCA variants struggled to model the curvature of the oral cavity on the first iterations, consequently affecting the fitness between the data and the quadratic model (Figure 3 and 4). Nevertheless, 10/15 models had a correlation $R^2 \geq 0.80$. The curvature (A), the height (C), and the symmetry (B and -B/2A) of each quadratic model was compared to the age, weight, and height of the corresponding case, hoping to reveal relevant trends. The greatest correlation was found between patient height and curvature (R^2=0.48), followed by weight and curvature (R^2=0.29), and trailed by the height and symmetry of the parabola (R^2=0.23 for B and R^2=0.20 for B/2A). Correlations were consolidated in Table 2. The value of B moves the maximum (or minimum) value of the model. The *x*-coordinate of said maximum is given by the ratio B/2A. Remaining correlations did not exceed R^2>0.15. Unavailable case information limited this analysis to a subset of the database.

TABLE 2: CORRELATIONS

	N	A	B	C	B/2A
Age (months)	*14*	0.06	0.15	0.05	0.01
Weight (Kgs.)	*13*	**0.29**	0.06	0.09	0.07
Height (cm.)	*11*	**0.48**	**0.23**	0.02	**0.20**

As we expand our database, we hope for correlations to strengthen or new parallels to arise. Current results point towards a lack of significant association between case parameters (patient's age, weight, and height) and our parabolic models. While this ultimately supports the need for patient-specific solutions, a few more cases could strengthen correlations beyond $R^2>0.75$. Even in this scenario, our results do show that height influences model parameters more so than weight, which is currently the metric for laryngoscope selection. Verathon® currently manufactures the Glidescope Spectrum series, a line of single-use laryngoscopes [8]. The series includes three pediatric sizes within their LoPro family, the LoPro S1, S2, and S2.5. According to Verathon®, the LoPro S1 is meant for patients ranging between 1.5 – 3.8 Kg., the S2 for 1.8 – 10 Kg., and the S2.5 for 10 – 28 Kg. We have shown that height may be a better parameters for classifying laryngoscope sizes. Based on our database, the variability in airway length renders the Verathon® classification inadequate for almost every patient in each group. For the first group, the LoPro S1 or simply the S1 group, a 3.8 Kg. infant had an estimated airway length of 19 mm, whereas the blade of the LoPro S1 extends to 29 mm. In the S2 group, two (2) patients featured 19 mm and 16.5 mm airways. These lengths better suit the LoPro S1 model but both patients weigh more than 5 Kg. The airway of the third patient was measured at 62 mm, making it a suitable candidate for the LoPro S2.5. However, the patient was only 9 Kg. Last but not least, 3/9 patients from the S2.5 group had airways shorter than the S2 blade (<44 mm) and 3/9 were 15 mm longer than the S2.5 blade (57 mm). All nine (9) patients ranged between 11 – 20 Kg. in weight. This comparison was consolidated in Figure 5. In this analysis, airway length was defined as the one-dimensional (1D) length between the oral cavity and the epiglottis, which was measured by both SCA variants.

CONCLUSIONS

The present work introduces a proof-of-concept method for the design and fabricate of patient-specific, pediatric laryngoscope blades. The method seeks to consolidate and automate reconstruction, segmentation, design, and fabrication processes currently disjointed and operator-dependent. We have begun validating our method by comparing results against industry standards. Furthering automation will rely on the correlation between patient-specific properties (extensive and/or intensive) and the method parameters (i.e. voxel size, dilation distance, intensity, etc.). Future work will also aim at developing physical models for validating fabricated patient-specific laryngoscope blades, perhaps leveraging novel high-fidelity,

multi-material printing and a strong collaboration between industry and academia.

Our method also served as an airway characterization tool. We will continue to expand our database and use our method to better understand changes in airway dimensions throughout development.
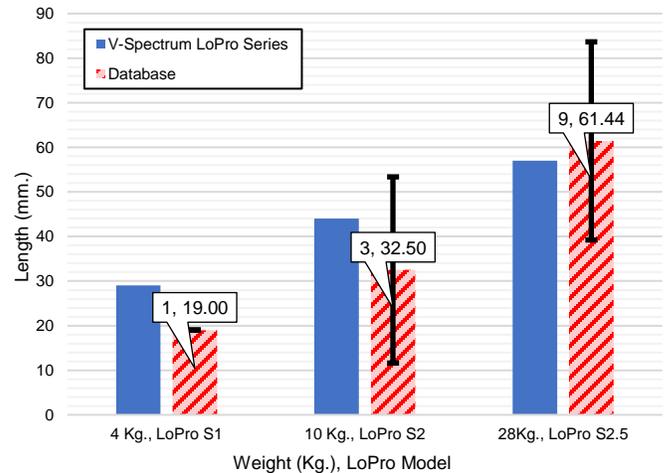

FIGURE 5: COMPARISON AGAINST STANDARD LARYNGOSCOPE MODELS

ADDITIONAL RESOURCES

We have consolidated our Patient-Specific Procedural Design Platform in a dedicated GitHub repository (https://github.com/pd3d/Houdini-Medical-Toolset).

REFERENCES

[1] Jane S. Doherty, Stephen R. Froom, Christopher D. Gildersleve. (2009). Pediatric laryngoscopes and intubation aids old and new. *Pediatric Anesthesia* Volume 19, Issue s1

[2] Savoldelli, G. L., Schiffer, E. , Abegg, C. , Baeriswyl, V. , Clergue, F. and Waeber, J. L. (2008), Comparison of the Glidescope®, the McGrath®, the Airtraq® and the Macintosh laryngoscopes in simulated difficult airways*. Anaesthesia, 63: 1358-1364. doi:10.1111/j.1365-2044.2008.05653.x

[3] Jodi Sherman. "Reusable vs. Disposable Laryngoscopes," Circulation 122,210, Volume 33, No 3, Anesthesia Patient Safety Foundation, February 2019

[4] M. Weiss and T. Engelhardt, "Proposal for the management of the unexpected difficult pediatric airway," *Pediatric Anesthesia,* no. 20, pp. 454-464, 2010.

[5] Christine E. Whitten. "10 Common Pediatric Airway Problems-And Their Solutions". August 10 2019

[6] Pydicom – Python package for working with DICOM files. https://pydicom.github.io/pydicom/stable/getting_started.html

[7] Runions, A., Lane, B. and Prusinkiewicz P., "Modeling Trees with a Space Colonization Algorithm," *Eurographics Workshop on Natural Phenomena, 2007.*

[8] Verathon – Glidescope Spectrum Single-Use https://www.verathon.com/glidescope-spectrum-single-use/